International Journal of Future Generation Communication and Networking
Vol. 13, No. 1, (2020), pp. 43-56

An Efficient and Robust Feature Extraction Based Biomedical Image Retrieval and Classification Model

C.Ashok kumar [1] and S.Sathiamoorthy[2]

[1] *Division of Computer and Information Science, Annamalai University, Annamalai Nagar, India*
[2]*Tamil Virtual Academy, Chennai,*
[1]*cashok1976@gmail.com,* [2]*ks_sathia@yahoo.com*

Abstract

Recently, there is an exponential growth in the number of medical images being generated from hospitals and medical organizations. Effective utilization of the images saved in the database for image retrieval and classification process becomes highly essential to accurately diagnose the patient and for further examination. In this view, this study presents new medical image retrieval and classification (MIRC) model, which retrieves the medical images related to the query image (QI) from the database and classifies the images. The proposed MIRC model involves three main processes namely feature extraction, image retrieval and image classification. At the initial stage, a set of two features namely texture and shape features get extracted from the input image. Then, the retrieval of the images takes place using a Euclidean distance based similarity measure. In line with, multilayer perceptron (MLP) based classification model is applied to classify the retrieved images. To improve the training process of MLP, hybridization of particle swarm optimization (PSO) and genetic algorithm (GA) is derived. During the testing phase, the proposed model determines the feature vectors of the test image and computes the similarity measure for retrieving the related images. Finally, the retrieved images undergo classification and allocate class labels to every test image. For validation, a set of benchmark NEMA CT images are employed. The experimental outcome clearly stated that the presented model has offered effective retrieval and classification performance by attaining maximum precision of 80.84%, recall of 86.49% and accuracy of 84.13%.

Keywords: — *Medical image retrieval, Classification, Feature extraction, Similarity measures*

1. Introduction

At present times, advanced development in the field of digital computer, multimedia, and storage models leads to massive image and multimedia content databases. Medical and diagnosis research works get advantageous from the advancements in digital storage and content processing. The medical organizations have the diagnosis and investigation facility, which generates massive quantity of imaging data which leads to an increased number of medical images. So, the design of efficient medical image retrieval model is needed to assist physicians to browse massive dataset. For handling the massive medical image database, several techniques for automated investigation of the medical images takes place [1–5]. A content based medical image retrieval (CBMIR) model is found to be an efficient model to diagnose and medicate different diseases and also a proficient management instrument [6] to handle massive dataset. With no use of these models, accessing, managing and extracting needed information from massive dataset is highly difficult. The process of retrieving medical images depending upon the textual details like tags and manual annotations leads to minimal outcome due to the requirement of man power, expert's analysis and time. So, it is needed to develop an effective CBMIR model which classifies and retrieves images in an automated way depending upon the extracted

features from the image. It finds helpful for clinical decision support system and research works to find related details from large repository.

Content based image retrieval (CBIR) is a computer vision approach which provides a method of looking for related images present in the massive database. The searching process depends upon the features of the image such as color, texture and shape or any other features extracted from the image. The effectiveness of a CBIR model is based on the chosen features [7]. The images are initially defined with respect to the features exist in a high dimensional feature space. Subsequently, the similarity between the images kept in a database and query image is determined in the feature space via a distance measure such as Euclidean distance. For this reason, for CBIR models, representing image data with respect to features and choosing a similarity measure is the significant element.

At present times, there is a rapid development in the area of machine learning (ML) modelsinspired from the concept human brain [8], which holds a detail of human brainand its process via many layers of transformation. Consequently, for learning features from the data in an automated way in multi levels of abstraction through the exploration of deep architectural models, ML approaches provides a straightaway approach for getting feature representation by enabling the model for learning complicated features from actual images with no use of hand crafted features.

Several research works have employed DL models for classification of retrieved medical images. In [7], a classification approach of benign and malignant breast lumps relied on shape parameters in sonography images is presented. [8] projected a clinical retrieval model for Diabetic Retinopathy(DR) as well as mammographic dataset. Also, it applied an optimized wavelet transform using a wavelet basis inside the lifting technique as well as assigning weights for every wavelet sub-bands. Alternate task which depends upon the wavelet transform for brain photography retrieval is explained in [9]. Hence, co-occurrence matrix dependent CT as well as MRI image retrieval has been projected in [10]. A rapid local-structure-based region-of-interest (ROI) retrieving technique for brain MRI photography is provided in [11]. In [12], a quantitative analysis is offered for pulmonary emphysema which can be seen in CT images of local binary pattern (LBP). It is applied in a combined manner as LBP, joint LBP as well as intensity histograms to characterize the ROIs.

[13] deployed a Uniformity Estimation Method (UEM) to obtain local intensity and textures to identify the pathological alteration in chest CT images. They have obtained the features by introducing an expansion of rotation invariant LBP as well as oriented variation in gradient vector to denote the intensity as well as image structure. [14] deployed a technique to retrieve 2D MRI images in the form of multimodal and noise control. The simulation outcome of 2D MRI brain photography is far better with respect to precision, speed, robustness multimodality and so on. Some other studies have also been presented in [15–18].

[15] developed a novel feature extraction method named as local co-occurrence ternary patterns (LTCoP) that is used in the encoding of the co-occurrence of same ternary edges from an image. With the provided central pixel, the measure of LTCoP could be estimated on the basis of first order derivatives from 8 dimensions. The addressed outcome depicts that, the quality of presented technique is effective when compared to other models such as LBP, local directional pattern (LDP), local ternary pattern (LTP) and so on. Afterwards, researchers established new feature description for biomedical image deriving model named as Local Mesh Patterns (LMeP) [16]. The LMeP is used to encode the association from enclosed neighbors of given reference image unlike to LBP, which encodes the correlation among predefined reference pixels as well as encircled neighbors. This model is expanded in [17] to get LMePVEP that is LMP valley edge patterns are

used. It has been revealed that LMePVEP depicts an enhancement with respect to ARR as well as ARP when related to LBP and its variants.

[19] designed a model named as Local Diagonal Extrema Pattern (LDEP) to retrieve CT images. It applies the first order derivatives to compute the measures of local diagonal extremas. Such indexes have been employed in creating a feature descriptor for the whole image. In order to illustrate the efficiency as well as quality of the technique, researchers related the final outcome with derived state-of-the-art techniques like LMeP, LTCoP, LTP, CSLBP, LBP and so on. It illustrates an enhancement in accuracy retrieval at the time of minimized processing duration. There is major advantage provided by LDEP than alternate techniques as it has minimized dimension of feature vector, by providing high computation under the application of minimum features.

This study presents an effective and robust medical image retrieval and classification (MIRC) model to retrieve the images relevant to the query image from the database and classifies it. The proposed MIRC model involves three main processes namely feature extraction, image retrieval and image classification. At the initial stage, a set of two features namely texture and shape features get extracted from the input image. Then, the retrieval of the images takes place using a Euclidean distance based similarity measure. Finally, multilayer perceptron based classification model is applied to classify the retrieved image which undergo training through the hybridization of particle swarm optimization (PSO) and genetic algorithm (GA), called as MLP-PSOGA. For validation, a set of benchmark NEMA CT images are employed. The comprehensive simulation outcome defined the superior characteristics of the presented model under several aspects over the existing methods.

The remaining portions of the study are arranged as follows. Section 2 presents the proposed MIRC approach. Section 3 validates the experimental analysis and Section 4 draws the conclusion.

2. The proposed MIRC model

The overall process involved in the proposed MIRC model has been displayed in Figure 1. As shown in Figure 1, the input image undergo a feature extraction phase which extracts a set of two distinct features namely texture and edges by the use of Directional local ternary quantized extrema patterns (DLTerQEPs) and Zernike Moments. Next to that, the similarity between the images kept in a database and that of a query image is determined in the feature space using Euclidean distance measure. Once the relevant images are retrieved, MLP-PSOGA based image classification takes place. The above-mentioned processes are clearly explained in the following subsections.

2.1.DLTerQEP based Texture Feature Extraction

DLTerQEP defines the spatial structure of local texture in ternary patterns by applying local extrema as well as dimensional geometric structures. In DLTerQEP, for a provided image, local extrema in every direction is required to be computed with local variation among intermediate as well as the adjacent pixels by indexing the patterns along pixel locations. The locations are indexed in the form of 4 directional extremas operator estimations. The Local Directional Extrema Values (LDEV) is applied for local patterns of an image and is estimated by the given Eq. (1):

$$LDEV(q,r) = \sum_{q=1}^{t_1}\sum_{r=1}^{t_1}[IG(q,r) - IG(1+floor(t_1/2), 1+floor(t_1/2))] \quad (1)$$

where, the input image has the size of $t_1 \times t_1$. The four directional, $HVDA_7$ structures of possible direction of LQP geometries are used in feature extraction task. The directional local extrema measures in $0°, 45°, 90°, 135°$directions has been extracted

in the form of $HVDA_7$ and filtered from LDEV valued as computed by Eq. (2). Then, 4 Directional Ternary Extrema Coding's (DTEC) are collected according to the four dimensions $(0°, 45°, 90°, 135°)$ from various thresholds with the help of LTP model. Thus, ternary coding patterns can be derived from the given function as:

$$DETC1(IG(gy_c))|_{\propto} =$$

$$\begin{cases} \vec{f_2}(LDEV(gy_{45}) \times LDEV(gy_{43}), IG(gy_c)); \vec{f_2}(LDEV(gy_{46}) \times LDEV(gy_{42}), IG(gy_c)); \vec{f_2}(LDEV(gy_{47}) \times LDEV(gy_{41}), IG(gy_c)); \propto = 0° \\ \vec{f_2}(LDEV(gy_{34}) \times LDEV(gy_{54}), IG(gy_c)); \vec{f_2}(LDEV(gy_{24}) \times LDEV(gy_{64}), IG(gy_c)); \vec{f_2}(LDEV(gy_{14}) \times LDEV(gy_{74}), IG(gy_c)); \propto = 45° \\ \vec{f_2}(LDEV(gy_{35}) \times LDEV(gy_{53}), IG(gy_c)); \vec{f_2}(LDEV(gy_{26}) \times LDEV(gy_{62}), IG(gy_c)); \vec{f_2}(LDEV(gy_{17}) \times LDEV(gy_{71}), IG(gy_c)); \propto = 90° \\ \vec{f_2}(LDEV(gy_{33}) \times LDEV(gy_{55}), IG(gy_c)); \vec{f_2}(LDEV(gy_{22}) \times LDEV(gy_{66}), IG(gy_c)); \vec{f_2}(LDEV(gy_{11}) \times LDEV(gy_{77}), IG(gy_c)); \propto = 135° \end{cases} \quad (2)$$

where $LDEV(gy_{ab})$= LDEV at (a,b) location of 7×7grid and gy_c is a gray metric of middle pixel. The upper LTP is filled with DTEC1 that is computed from Eq. (2) and using the measure of ($\vec{f_2}$) as provided below:

$$\vec{f_2}(a, gy_c) = \begin{cases} 1, if\ (a \geq (threshold = 2)); \\ 0, if\ (a < (threshold)); \end{cases} \quad (3)$$

Similarly, from Eq. (2), lower LTP, DTEC2 have been measured by obtaining the given value of ($\vec{f_2}$) as follows:

$$\vec{f_2}(a, gy_c) = \begin{cases} 1, if\ (a \geq (threshold = -2)); \\ 0, if\ (a < (threshold)); \end{cases} \quad (4)$$

The DTEC is derived from the Eqs. (2) - (4) are given below:

$$DETC(IG(gy_c)) = \begin{bmatrix} DTEC1(IG(gy_c))|_{0°}, DTEC1(IG(gy_c))|_{45°}, DTEC1(IG(gy_c))|_{90°}, DTEC1(IG(gy_c))|_{135°}; \\ DTEC2(IG(gy_c))|_{0°}, DTEC2(IG(gy_c))|_{45°}, DTEC2(IG(gy_c))|_{90°}, DTEC2(IG(gy_c))|_{135°} \end{bmatrix} \quad (5)$$

The DTEC coding is classified as two binary codes: upper LTP code as well as lower LTP code as similar to LTP. Practically, DLTerQEP allows the integration of tetra directional extremas of P=12-bit (w=0...11), and binary coding string generation for every binary pattern of LTP. By increasing the binomial weights for each DTEC LTP coding, a single DLTerQEP measures for particular pattern (7 × 7) characterizes the spatial structure of local pattern which can be defined using Eq. (6):

$$DLTerQEP_{\propto,P} = \sum_{w=0}^{P-1} DTEC_{(upper\ /lower\ ),}\ w2^w \quad (6)$$

From the entire image, each DTECLTP map presented is in the range of 0 to 4095 (0 to 2^P -1), as a result, the overall DTECLTP map is developed along with the previous value of 0 to 8191 (0 to ((2(2^P))-1). The DLTerQEPs is totally varied from LBP method. It extracts the spatial association from the set of adjacent values from local regions including the directions allocated, and LBP is isolated using the correlation from middle as well as neighboring pixels. It consumes the directional edge data on the basis of local extrema.

2.2.Zernike Moments (ZM) based Edge Feature Extraction

Medicinal image like CT as well as MRI images are comprised of different features like textures, shape and so on. The biomedical image retrieving technique involves images from various parts of human body. The overall view of such images is significant for unambiguous distinction between them. As the localized features

are not capable of holding the major factor of an image, ZMs has been employed, which has been allocated as global descriptor for medicinal images retrieving system.In this study, ZM is employed as shape descriptors and identified as rotation invariant because of Orthogonality characteristic.

Here, ZMs are applicable in holding required features. The property of orthogonality from ZMs is useful to attain the neighbor value zero of redundancy from the calculated set of ZMs coefficients, thus the moment rates at diverse orders denotes a unique as well as independent features of an image. It is named as global feature descriptors as it act obtains statistical distribution of pixel data inside the lower influenced shape. In addition, ZMs are estimated as a consequence of summation; hence, the impact of noise in a magnitude of ZMs coefficients is negligible. Here, ZMs [21] are assumed to be the orthogonal moments that are derived by applying the input image into difficult orthogonal Zernike polynomials. Also, ZMs of order a as well as standard b of a function f(u,v) across a unit disk are described by

$$Z_{ab} = \frac{a+1}{\pi} \iint_{u^2+v^2 \le 1} f(u,v) Y_{ab}^{*}(u,v) du dv \tag{7}$$

where a signifies a non-negative integer, b denotes the integer of 0≤|b|≤a, and a-|b|=even. The expression of $\boldsymbol{Y_{ab}^{*}}$ (u, $\boldsymbol{v}$) is more tedious to combine with Zernike orthogonal basis function $\boldsymbol{Y_{ab}}$(u,v) that is expresses as:

$$Y_{ab}(u,v) = Y_{ab}(r,\theta) = R_{ab}(r) \exp(nb\theta) \tag{8}$$

where $r = \sqrt{u^2+v^2}, \theta = \tan^{-1}\left(\frac{v}{u}\right), 0 \le \theta \le 2\pi, n = \sqrt{-1}$

The radial polynomial $Rabr$ is given as follows:

$$R_{ab}(r) = \sum_{s=0}^{(a-|b|)/2} (-1)^s \frac{(a-s)!}{s!\left(\frac{a+|b|}{2}-s\right)!\left(\frac{a-|b|}{2}-s\right)!} (r)^{a-2s} \tag{9}$$

Zeroth order approximation of Eq. (9) is provided as

$$Z_{ab} = \frac{2(a+1)}{\pi J^2} \sum_{m=0}^{J-1} \sum_{k=0}^{J-1} f(u_m, v_k) R_{ab}(r_{mk}) e^{-nb\,\theta_{mk}} \tag{10}$$

where (l_m, v_k) refers the general coordinate position of its own pixel (m,k) that is derived by using the coordinate conversion:

$$u_m = \frac{2m+1-J}{J\sqrt{2}}, v_k = \frac{2k+1-J}{J\sqrt{2}} \tag{11}$$

for every m, k=0,1 ,2,...,J-1. The external unit disk of ZMs determining that offers optimal function for ZMs-based image pattern mapping issues [44, 45]. Additionally, the presented models of ZMs-relied model does not apply the moments with negative b, due to the presence of $|Z_{a,b}| = |Z_{a-b}|$.

2.3. Euclidean distance based Similarity measurement

In CBMIR model, Euclidean distance is applied to find the similarity exist among the images. The distance between the two images are used for determining the similarity among the images. Euclidean distance is an important distance measure. It is determined by the use of Minkowski Distance formula by setting p's value to 2. For any two images x and y,it will update the distance 'd' as given as

$$d(x,y) = \sqrt{\sum_{i=1}^{n}(x_i - y_i)^2} \quad (12)$$

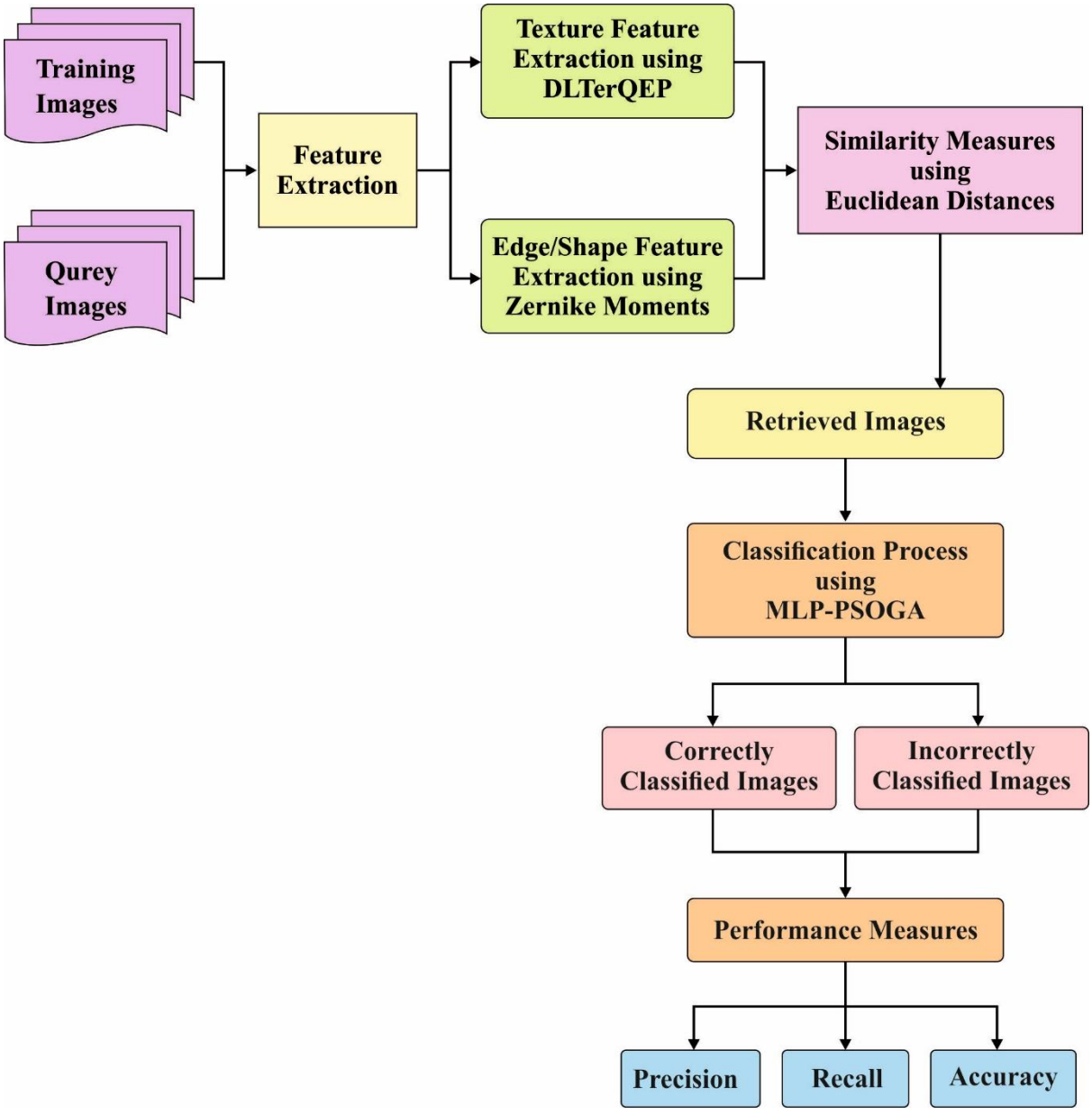

Figure 1. Overall process of proposed MIRC model

2.4. MLP-PSOGA based classification

Once the images are retrieved, classification of images takes place. MLP belongs to the category of feed forward Artificial Neural Network (ANN) with a set of 3 layers. The primary infrastructure of MLP is shown, where x, h and y denotes the count of input, hidden as well as output nodes correspondingly. In this study, every weight of MLP has been saved in the form of matrix W and each bias is recorded in matrix B. Initially, sum of weighted inputs are estimated as

$$s_v = \sum_{u=1}^{n} \left(W\left((v-1)x+u\right) * X_x\right) + B(v), v = 1, 2, \cdots, h \quad (13)$$

W((v- 1) x+u) signifies the weight derived from ith input node to jth hidden node, B(v) implies the biasing of jth hidden node and X_x refers as ith input. The weights as well as biases are projected in the form of matrix as the way it is saved in a matrix. The result from every hidden node is expressed as.

$$S_v = \text{sigmoid}(s_v) = \frac{1}{\left(1 + \exp(-s_v)\right)}, v = 1, 2, \cdots, h \quad (14)$$

Finally, the outcome is measured as

$$o_k = \sum_{v=1}^{h} (W(xh + (k-1)h + v) * S_v) + B(h+k), k = 1, 2, \cdots, y \quad (15)$$

$$O_k = \text{sigmoid}(o_k) = \frac{1}{\left(1 + \exp(-o_k)\right)}, k = 1, 2, \cdots, y \quad (16)$$

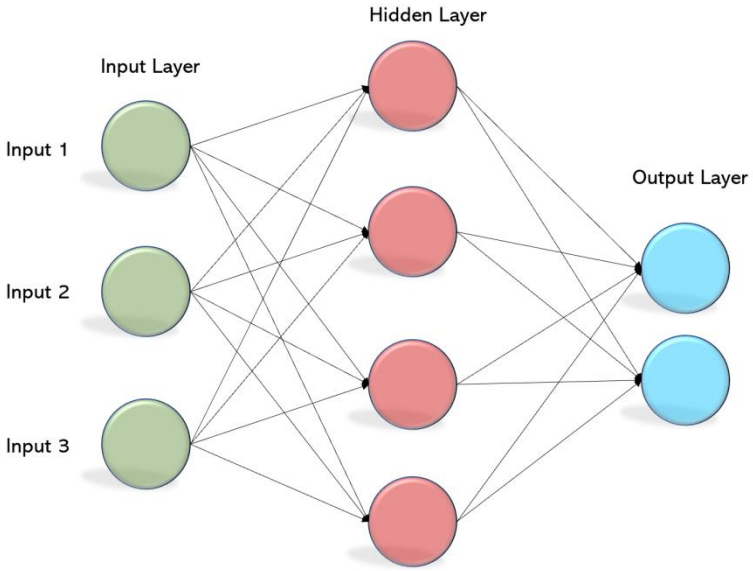

2.5.

Figure 2. Structure of MLP

$W(xh + (k-1)h + v)$ indicates the weight from jth hidden layer to kth node of output layer, and B(h+k) is a bias of kth output node. The major operation in training MLP is the process of obtaining optimized conjunction of weight and bias to retrieve desired result from the provided inputs. Each weight as well as bias is combined to make a candidate from a population that is every weight and bias is considered to a parameter of candidate solution.

$$\text{Candidate Solution} = \{W(1), W(xh + yh), B(1), \ldots\ldots, B(h + y)\} \quad (17)$$

The total count of weights must undergo optimization xh+y has well as total biases should also be optimized is h+y. Hence, number of variables in training MLP is (x+1)h+(h+1)y. Usually, architecture of MLP is implied as x−h−y. The input layer nodes are similar as features applied for classification issue. The number of hidden nodes can be defined as

$$H = 2XN + 1 \quad (18)$$

where N= Number of input nodes and H= Number of hidden nodes. It is proven that, total number of weights and biases to be optimized is directly proportional to the number of features. Since feature count in a problem gets increased, the MLP becomes big and consequently makes the search space highly difficult. To overcome this issue, the training process of MLP takes place by the use of PSOGA model.At this point, the hybridization of PSO and GA takes place. Once the population is initialized using N particles and measuring the fitness for all particles, only the better N/2 particles are induced to PSO. It then concludes in PSO and again provided to GA. Consequently, the simulation outcome of PSO as well as GA has been concatenated to make N particles. Further, N/2 best particles have been chosen from N particles which are used for upcoming generation. Fig. 3 illustrates the process involved in PSOGA. The technical steps of PSOGA are used to train an n-h-m MLP as provided as follows:

Step 1: Random population initialization with every particle having (xh+yh)+(h+y) attributes. Initialization of velocity takes place with respective to every particle. N= Size of population.

Step 2: Assume Inertia weight, Acceleration constant, Crossover type, Selection type, Crossover Probability, Mutation Probability, and Maximum generation count.
Step 3: Determine MSE for every particle in the population using forward pass functions on MLP.

Step 4: Choose optimal N/2 particles/individuals and abandon the worse half.

Step 5: Compute pbest and gbest solutions.

Step 6: Updating particle velocities.

Step 7: Updating particle positions.

Step 8: Estimate MSE for every particle in the population using forward pass functions on MLP.

Step 9: Updating pbest as well as gbest solutions.

Step 10: Determine the fitness value of every individual.

Step 11: With respect to fitness value, select the best half of the population.

Step 12: With respect to Crossover type and Crossover Probability, execute crossover function among the selected individuals.

Step 13: Execute mutation function.

Step 14: Substitute the worse half through new children produced from Steps 11-13.
Step 15: Merge population (Total N particles/individuals).

Step 16: Ensure the completion of maximum iteration count. If yes, display the optimal individual of present population as outcome. Else, jump to Step 4.

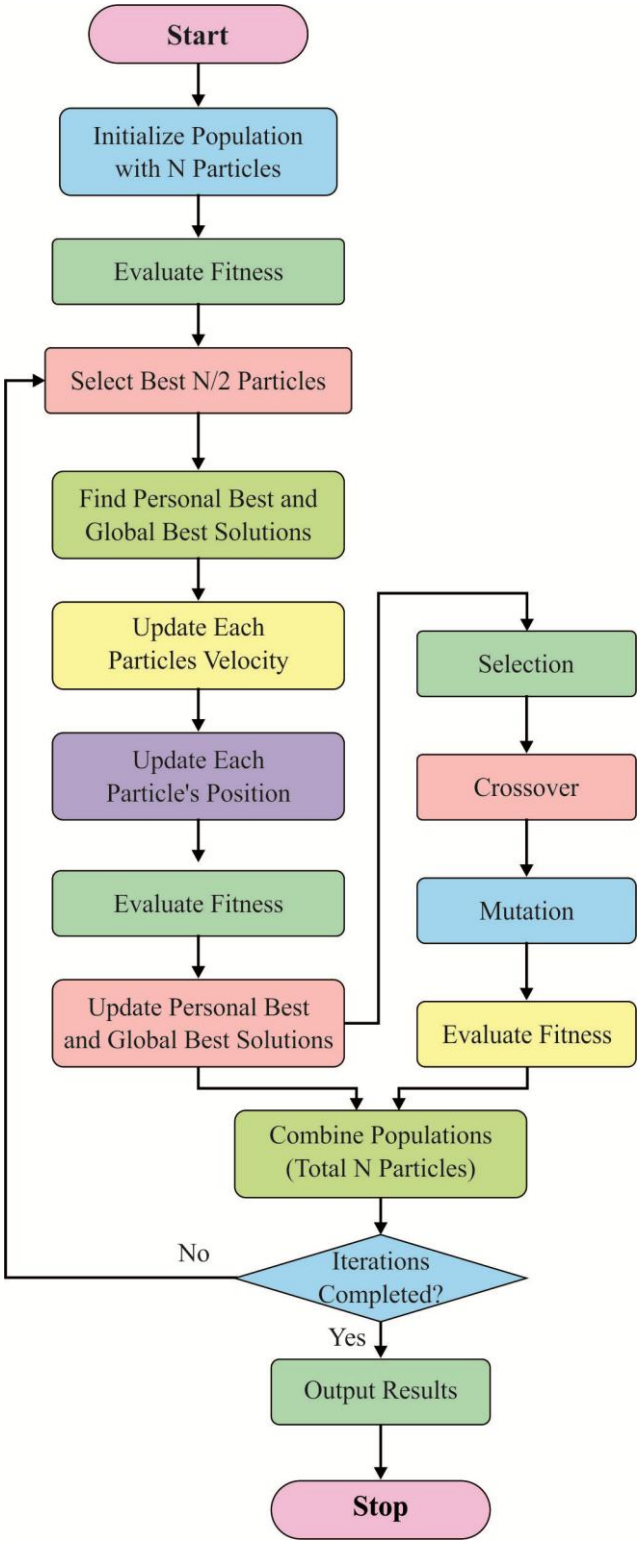

Figure 3. Flowchart of PSOGA

3. Performance Validation

3.1 Dataset used

For verifying the effective results of the presented MIRC model, a benchmark NEMA CT images has been employed which holds different parts of human [17]. It provides precise information representation ability to accuratelydistinguish the images which are comprised in the whole representation, i.e. global scale. The information related to the employed NEMA CT dataset are given in Table 1, comprising a set of 600 images with the pixel dimensions of 512*512. Besides, a set of ten classes were exist in the whole dataset. A set of sample test images are also provided in Figure 4.

Table 1 Dataset Description

Description	Values
Database	NEMA CT
Number of Images	600
Image Size	512*512
Number of Classes	10
Classes Distribution	54, 70, 66, 50, 15, 60, 52, 104, 60, 69

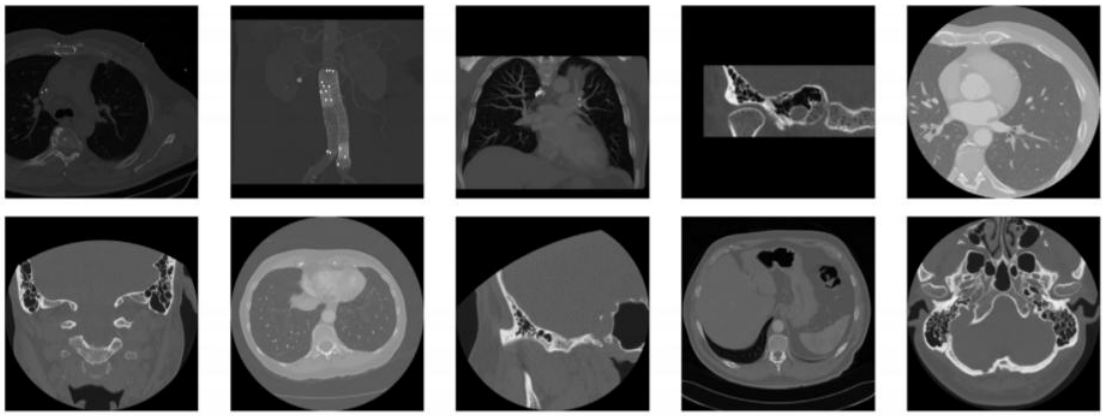

(a)

Figure 4. Sample Test Images

3.2 Results Analysis

An extensive comparative study is made between the presented MIRC model and existing models as shown in Table 1. Figure. 5-7 shows the results analysis of diverse models interms of precision, recall and accuracy respectively. By examining the outcome of the presented MIRC model on the test dataset interms of precision, it is shown that a set of three models namely LTDP, LQEP and LMeP models achieves minimal precision values of 8.97%, 8.93% and 8.91% respectively. On continuing with, a slightly better outcome is offered by the LDEP, DLTerQEP and LDGP models by achieving near identical prevision values of 10.27%, 9.10% and 10.27%. Simultaneously, the LWP and LBDP models exhibits manageable and closer precision values of 31.03% and 32.57%. In the same way, the OFMM and PSO-SVM models provides near optimal classification outcome by offering a higher precision value of 48.51% and 53.67%. However, the presented model offered maximum results by achieving optimal precision value of 80.84%.

Table 1 Comparison of different models under diverse measures

Methods	Precision	Recall	Accuracy
Proposed	**80.84**	**86.49**	**84.13**
PSO+SVM	53.67	77.89	65.38
OFMM	48.51	74.12	60.52
LBDP	32.57	47.11	40.61
LWP	31.03	46.51	38.54
LDEP	10.27	18.39	15.96
DLTerQEP	09.10	16.68	13.62
LDGP	09.05	17.28	13.51
LTDP	08.97	16.59	12.94
LQEP	08.93	16.55	12.85
LMeP	08.91	16.66	12.64

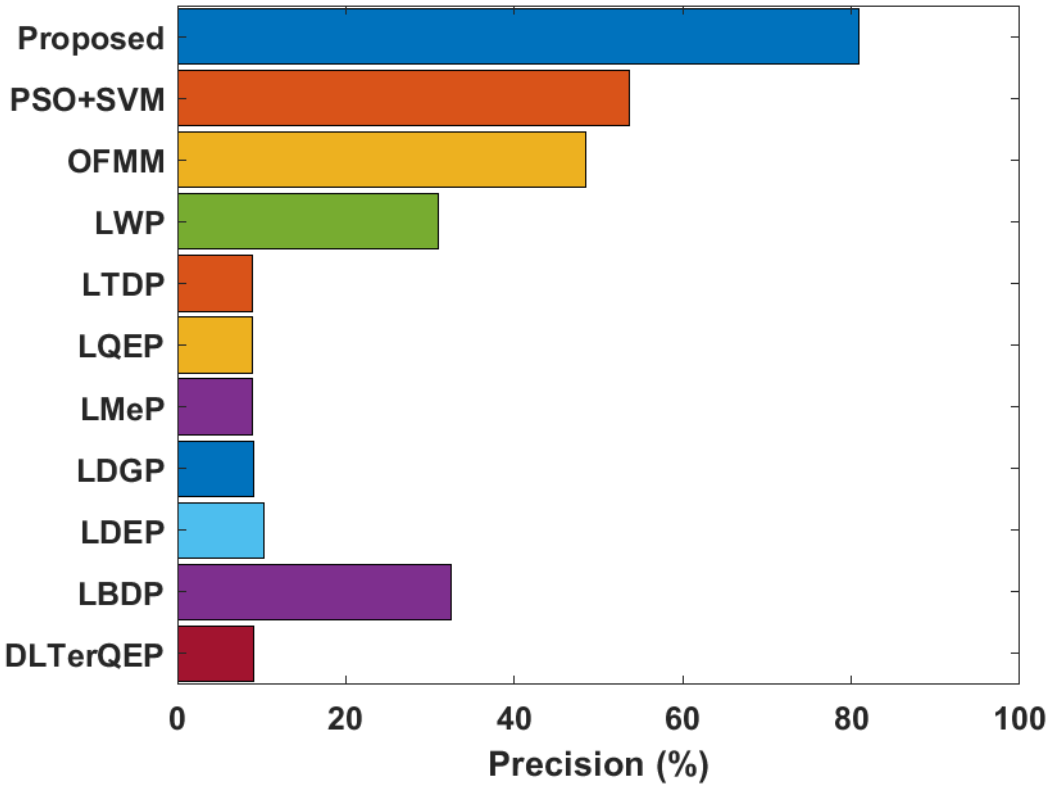

Figure 5.Precision analysis of diverse models

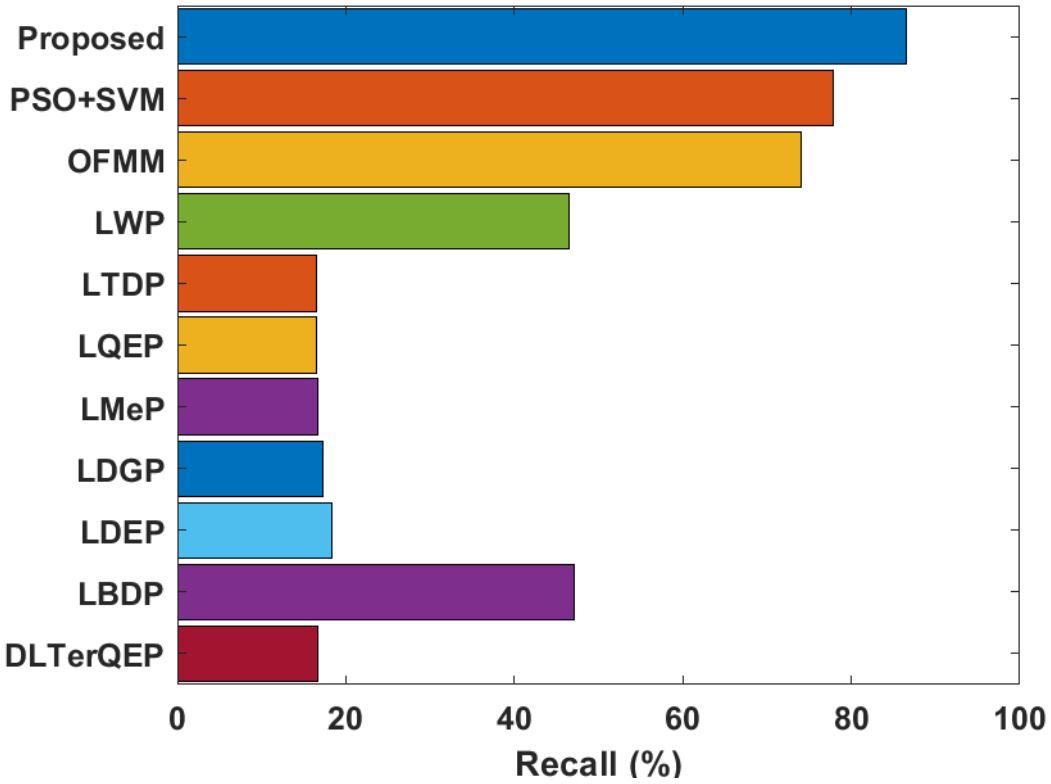

Figure 6.Recall analysis of diverse models

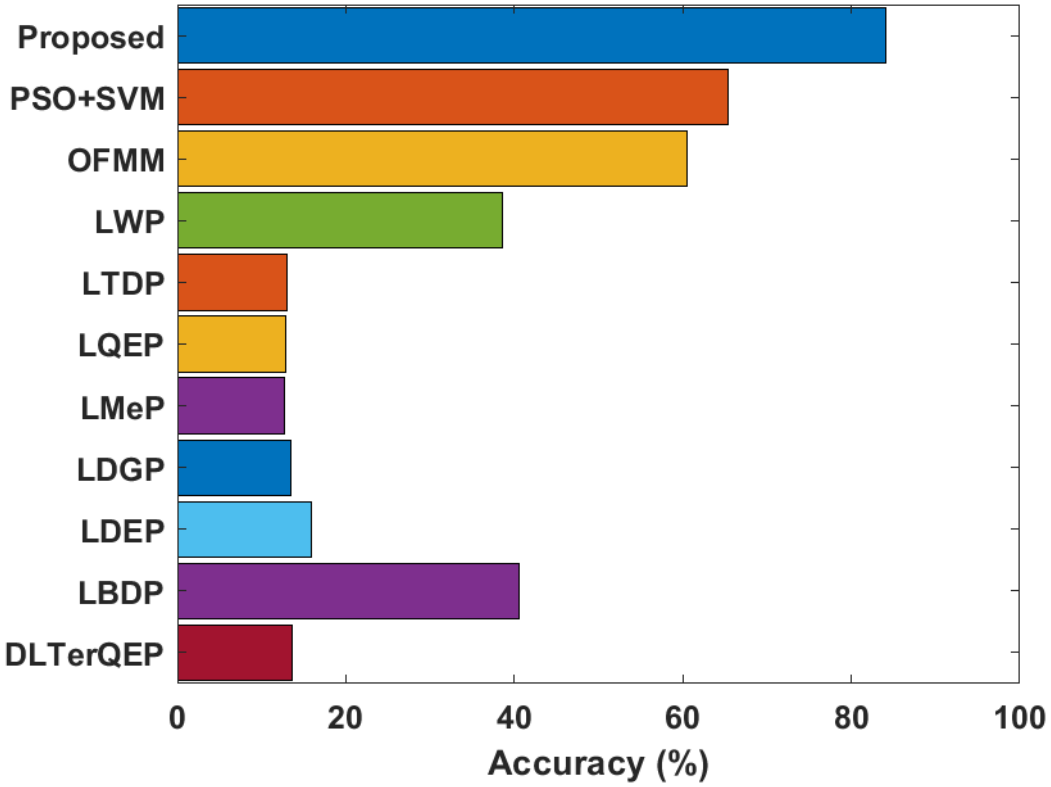

Figure 7.Accuracy analysis of diverse models

On determining the classifier results interms of recall, it is shown that a set of four models namely DLTerQEP LTDP, LQEP and LMeP models has offered ineffective classification outcome by achieving recall values of 16.68%, 16.59%, 16.55% and 16.66% respectively. After that, a slightly better outcome is offered by the LDEP and LDGP models by achieving near identical recall values of 18.39% and 17.28%. Simultaneously, the LWP and LBDP models exhibit manageable and closer recall values of 46.51% and 47.11%. In the same way, the OFMM and PSO-SVM models provides near optimal classification outcome by offering a higher recall value of 74.12% and 77.89%. However, the presented model offered maximum results by achieving optimal recall value of 86.49%.

On comparing the results offered by the proposed model interms of accuracy, it is depicted that LTDP, LQEP and LMeP models achieves minimal accuracy values of 12.94%, 12.85% and 12.64% respectively. Then, a slightly better outcome is offered by the LDEP, DLTerQEP and LDGP models by achieving near identical accuracy value of 15.96%, 13.62% and 13.51%. At the same time, the LWP and LBDP models exhibit manageable and closer accuracy values of 38.54% and 40.61%. In the same way, the OFMM and PSO-SVM models provides near optimal classification outcome by offering a higher accuracy value of 60.52% and 65.38% respectively. However, the presented model offered maximum results by achieving optimal accuracy value of 84.13%.

After looking into the above mentioned table and figures, it is clearly ensured that the presented MIRC model has offered supreme retrieval and classification performance under several aspects.

4. Conclusion

This paper has introduced an effective MIRC model to effectively retrieve the images from databases and classify the images in an appropriate way. The presented model has incorporated three main stages namely feature extraction (texture and edge/shape), image retrieval using Euclidian distance, and MLP-PSOGA based classification. Upon providing a new test medical image, the proposed model determines the feature vectors and similarity measure for retrieving the related images. At last, the retrieved images have undergone classification and allocated class labels to every test image. For validation, a set of benchmark NEMA CT images are employed. The experimental outcome clearly stated that the presented model has offered effective retrieval and classification performance by attaining maximum precision of 80.84%, recall of 86.49% and accuracy of 84.13%. The simulation results ensured that the presented model can be deployed in real time environment to retrieve images from hospital databases and classifies it.

References

[1] Y. Rui, T.S. Huang, Image retrieval: current techniques, promising directions and open issues, J. Vis. Commun. Image Representation 10 (1999) 39–62.
[2] A.W.M. Smeulders, M. Worring, S. Santini, A. Gupta, R. Jain, Content-based image retrieval at the end of the early years, IEEE Trans. Pattern Anal. Mach. Intell. 22 (2000) 1349–1380.
[3] M. Kokare, B.N. Chatterji, P.K. Biswas, A survey on current content based image retrieval methods, IETE J. Res. 48 (2002) 261–271.
[4] Y. Liu, D. Zhang, G. Lu, W.-Y. Ma, A survey of content-based image retrieval with high-level semantics, Pattern Recogn. 40 (2007) 262–282.
[5] [5] H. Muller, N. Michoux, D. Bandon, A. Geisbuhler, A review of content-based image retrieval systems in medical applications—Clinical benefits and future directions, Int. J. Med. Inf. 73 (2004) 1–23.
[6] K.N. Manjunath, A. Renuka, U.C. Niranjan, Linear models of cumulative distribution function for content-based medical image retrieval, J. Med. Syst. 31 (2007) 433–443
[7] F.S. Zakeri, H. Behnam, N. Ahmadinejad, Classification of benign and malignant breast masses based on shape and texture features in sonography images, J. Med. Syst. 36 (2010) 1621–1627.
[8] G. Quellec, M. Lamard, G. Cazuguel, B. Cochener, C. Roux, Wavelet optimization for content-based image retrieval in medical databases, J. Med. Image Anal. 14 (2010) 227–241.

[9] A.J. Traina, C.A. Castanon, C. Traina Jr, Multiwavemed: a system for medical image retrieval through wavelets transformations, in: Proceedings of the 16th IEEE Symposium on Computer-Based Medical Systems, New York, USA, 2003, pp. 150–155.
[10] J.C. Felipe, A.J. Traina, C. Traina Jr, Retrieval by content of medical images using texture for tissue identification, in: Proceedings of the 16th IEEE Symposium on Computer-Based Medical Systems, New York USA, 2003, pp. 175–180.
[11] D. Unay, A. Ekin, R.S. Jasinschi, Local structure-based region-of interest retrieval in brain MR images, IEEE Trans. Inf. Technol. Biomed. 14 (2010) 897–903.
[12] L. Sørensen, S.B. Shaker, M. de Bruijne, Quantitative analysis of pulmonary emphysema using local binary patterns, IEEE Trans. Med. Imaging 29 (2010) 559–569.
[13] S.H. Peng, D.H. Kim, S.L. Lee, M.K. Lim, Texture feature extraction based on uniformity estimation method for local brightness and structure in chest CT images, Comput. Biol. Med. 40 (2010) 931–942.
[14] A. Quddus, O. Basir, Semantic image retrieval in magnetic resonance brain volumes, IEEE Trans. Inf. Technol. Biomed. 16 (2012) 348–355.
[15] S. Murala, Q.M.J. Wu, Local ternary co-occurrence patterns: a new feature descriptor for MRI and CT image retrieval, Neurocomputing 119 (2013) 399–412.
[16] S. Murala, Q.M.J. Wu, Local mesh patterns versus local binary patterns: biomedical image indexing and retrieval, IEEE J. Biomed. Health. Inf. 18 (2014) 929–938.
[17] S. Murala, Q.M.J. Wu, MRI and CT image indexing and retrieval using local mesh peak valley edge patterns, Signal Process. Image Commun. 29 (2014) 400–409.
[18] S. Murala, Q.M.J. Wu, Spherical symmetric 3D local ternary patterns for natural, texture and biomedical image indexing and retrieval, Neurocomputing 149 (2015) 1502–1514
[19] S.R. Dubey, S.K. Singh, R.K. Singh, Local diagonal extrema pattern: a new and efficient feature descriptor for CT image retrieval, IEEE Signal Process Lett. 22 (2015) 1215–1219.

Authors

C.Ashok kumar, received MSc (IT) degree from Madras University and M.Phil degree from Bharathidasan University, India. He joined in the Annamalai University in the year 2005. At present he is working in the Department of Computer Science, Dr.MGR Arts & Science College, Villupuram. He has almost 14 years of teaching experience. He is currently pursuing Ph.D degree in the Department of Computer and Information Science, Annamalai University. His research interests include Pattern Recognition and Image Retrieval.

S.Sathiamoorthy, received B.Sc degree in Physics from University of Madras, M.C.A degree from Bharathidasan University and M.Phil as well as Ph.D. from Annamalai University, India. In the year 2001, he joined in the Department of Computer Science and Engineering, Annamalai University and also served in the Computer Science and Engineering Wing of Directorate of Distance Education and Department of Computer and Information Science, Annamalai University. At present, he is Assistant Director (Controller of Examinations), Tamil Virtual Academy, Information Technology Department of Tamil Nadu Government, India. He has almost 19 years of teaching experience. Currently he is working on Pattern recognition, Pattern analysis, Image retrieval and classification. His research interests include Machine learning algorithms and Medical image analysis. He has published more than 30 papers in various International journals and more than 20 papers in National and International conferences. He has been on the reviewing and editorial board of many reputed journals.